Quantum interference by coherence transfer from spin to orbital angular momentum of photons

Nagali E.[a], Sciarrino F.[a], Sansoni L.[a], De Martini F.[a,b], Marrucci L.[c,d], Piccirillo B.[c,d], Karimi E.[c] and Santamato E.[c,d]

[a]Dipartimento di Fisica dell'Università "La Sapienza" and Consorzio Nazionale Interuniversitario per le Scienze Fisiche della Materia, Roma 00185, Italy;
[b]Accademia Nazionale dei Lincei, via della Lungara 10, Roma 00165, Italy;
[c] Dipartimento di Scienze Fisiche, Università di Napoli "Federico II", Compl. Univ. di Monte S. Angelo, 80126 Napoli, Italy;
[d] CNR-INFM Coherentia, Compl. Univ. di Monte S. Angelo, 80126 Napoli, Italy

ABSTRACT

The orbital angular momentum carried by single photons represents a promising resource in the quantum information field. In this paper we report the characterization in the quantum regime of a recently introduced optical device, known as *q-plate*. Exploiting the spin-orbit coupling that takes place in the q-plate, it is possible to transfer coherently the information from the polarization to the orbital angular momentum degree of freedom, and *viceversa*. Hence the q-plate provides a reliable bi-directional interface between polarization and orbital angular momentum. As a first paradigmatic demonstration of the q-plate properties, we have carried out the first experimental Hong-Ou-mandel effect purely observed in the orbital angular momentum degree of freedom.

Keywords: Orbital angular momentum, entanglement, Hong-Ou-Mandel effect

1. INTRODUCTION

In the last few decades, quantum optics has allowed the implementation of a variety of quantum-information protocols. However, the standard information encoding based on the two-dimensional quantum space of photon polarizations (or "spin" angular momentum) imposes significant limitations to the protocols that may be implemented. To overcome such limitations, more recently the orbital angular momentum (OAM) of light, related to the photon's transverse-mode spatial structure,[1] has been recognized as a new promising resource, allowing the implementation of a higher-dimensional quantum space, or a "qu-dit", encoded in a single photon.[2,3] Related to its higher dimensionality, the OAM can provide an elevated degree of security and higher information-density coding, with a major channel capacity in the field of quantum communication.[4,5] Furthermore, it can be exploited in quantum imaging, free-space communication, micromechanics, astrophysics and biophysics.[3,6–8]

Single photons carry angular momentum both with a spinoral and orbital contributions, which can be treated independently in paraxial approssimation.[9] The wavefront of light carrying OAM shows a twisting around the propagation direction (elicoidal wavefront), which causes a phase singularity known as optical vortex. The handness and the number of twisting define the value of an integer number m that represents the eigenvalue of the orbital angular momentum (in unit of $\hbar$) carried by each photon of the light beam. One of the most popular class of light field carrying OAM is the Laguerre-Gauss beam,[1] characterized by the dependence of the modes on the azimuthal phase ϕ in the expression $e^{im\phi}$. Such dependence implies that the Laguerre-Gauss modes are eigenmodes of the quantum orbital angular momentum operator $\hat{L}_z|m\rangle = m\hbar|m\rangle$ and form a complete basis in the Hilbert space. This property suggested an employment of OAM states in quantum field. So far, the generation of OAM-entangled photon pairs has been carried out by exploiting the process of parametric down-conversion[10,11] and has also been utilized in few quantum information protocols.[12,18,19] Despite these successes, the optical tools for generating and controlling the OAM photon states (computer-generated holograms, Dove's prisms, cylindrical lens mode converters, etc.) are rather limited. A convenient way to coherently "interface" the OAM degree of freedom of photons with the more easily manipulated spin/polarization one has been missing so far. In this context, the recent invention of an optical device, the so-called "q-plate" (QP), that couples the

Photon Counting Applications, Quantum Optics, and Quantum Information Transfer and Processing II, edited by Ivan Prochazka, Roman Sobolewski, Miloslav Dusek, Proc. of SPIE Vol. 7355, 735507
 · doi: 10.1117/12.821083

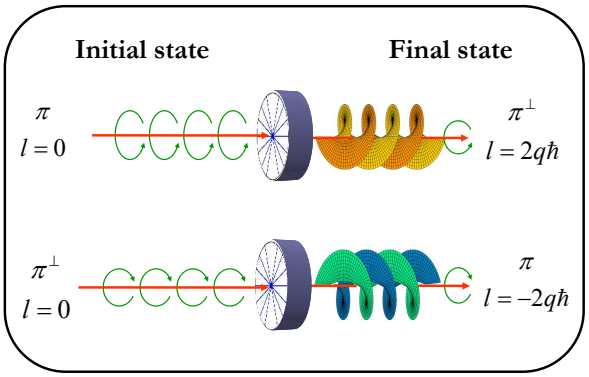

Figure 1. Dynamic on single-photon states induced by the q-plate.

photon spin to its orbital angular momentum opens up a number of new and unexplored possibilities.[20] This optical "spin-orbit" coupling can be exploited as an effective interface, completely reversible, between polarization and orbital angular momentum in the quantum regime.[23]

In this paper we present the characterization of the q-plate properties in the quantum regime, enlightening its reliability in transposing the quantum information from the spin to the OAM degree of freedom of photons and *vice versa*.[23,27] Finally, we demonstrate experimentally that photon-photon quantum correlations can be transferred from the spin to the OAM degree of freedom of a photon pair, through the observation of a Hong-Ou-Mandel effect in the OAM.

The ease of use, flexibility and good conversion efficiency demonstrated by this device makes it a promising tool for exploiting the OAM degree of freedom of photons, in combination with polarization, as a resource to implement high-dimensional quantum information protocols.

2. THE Q-PLATE DEVICE

A q-plate (QP) is a birefringent slab having a suitably patterned transverse optical axis, with a topological singularity at its center.[20] The "charge" of this singularity is given by an integer or half-integer number q, which is determined by the (fixed) pattern of the optical axis. Q-plates working in the visible or near-infrared domain can be manufactured with nematic liquid crystals, by means of a suitable treatment of the containing substrates.[20,21] The q-plate introduces a birefringent retardation δ which is uniform across the device. For $\delta = \pi$, a QP modifies the OAM state m of a light beam crossing it, imposing a variation $\Delta m = \pm 2q$ whose sign depends on the input polarization, positive for left-circular and negative for right-circular.[22] In other words, the input polarization of the light controls the sign of the orbital helicity of the output wave front. We observe that the total variation of the angular momentum of light is nil, and there is no net transfer of angular momentum to the plate: the plate in this case acts only as a coupler of the two forms of optical angular momentum, allowing their conversion into each other. In the present work, we use only QPs with charge $q = 1$ and $\delta \simeq \pi$. Hence, an input TEM_{00} mode (having $m = 0$) is converted into a beam with $m = \pm 2$, as shown in Fig. 1. In the visible domain, in particular ate $\lambda = 795$nm, we have extimated the transmittivity of the q-plate to be $T \sim 0.90$.[23]

Let us now describe the action of the q-plate adopting the quantum formalism between the input and output modes. In a single-photon quantum formalism, the QP implements the following quantum transformations on the single photon state:

$$\begin{aligned} |L\rangle_\pi |m\rangle_o &\rightarrow |R\rangle_\pi |m+2\rangle_o \\ |R\rangle_\pi |m\rangle_o &\rightarrow |L\rangle_\pi |m-2\rangle_o \end{aligned} \quad (1)$$

where $|\cdot\rangle_\pi$ and $|\cdot\rangle_o$ stand for the photon quantum state 'kets' in the polarization and OAM degrees of freedom, and L and R denote the left and right circular polarization states, respectively. Since the previous relations hold for single photon creation operators, it emerges the possibility to exploit the q-plate in the quantum regime. Let us note that a single q-plate with $q = 1$ allows to manipulate the OAM degree of freedom in the subspace o_2. In the following, whenever there is no risk of ambiguity, the subscripts π, o and o_2 will be omitted for brevity.

Let us address how to optimize the efficiency of the q-plate. The birifringence retardation δ introduced by the q-plate is function of $\frac{\Delta n L}{\lambda}$, where L is the QP thickness, λ the wavelenght and Δn the liquid crystal birefringence. Hence the efficiency η of the device, which can be expressed as $\eta = \sin^2 \frac{\delta}{2}$, depends critically on the pressure acting on the q-plate and on the working temperature, since these parameters can modify the thickness and the birefringence, respectively. The q-plate conversion efficiency η from the input TEM_{00} to the $m = \pm 2$ modes

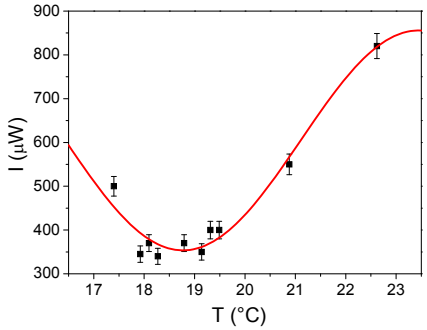

Figure 2. Experimental analysis of the conversion efficiency of the q-plate depending on the temperature. The optimal tuning of the QP corresponds to a birefringence retardation $\delta = \pi$, hence the QP acts as a half waveplate on the polarization. The data correspond to the intensity transmitted by a PBS placed after the QP, while varying the working temperature. The input beam has been injected on the QP with horizontal polarization and decentralized respect to the singularity. Lower the intensity transmitted, better is the tuning of the QP, that is the efficiency of conversion. The solid line refers to the sinusoidal best fit.

can be estimated through the coupling efficiency with the single mode fiber. Experimentally we find $\eta \simeq 85\%$. This is mainly ascribed to the fact that our q-plate has a birefringent retardation δ not exactly tuned to π and the unconverted component remains $m = 0$ and is therefore filtered out. In order to optimize the QP efficiency, we have estimated its temperature dependence. By mounting the q-plate on a termo-electric cooler connected to a temperature controller, we have observed a sinusoidal efficiency behaviour depending on the temperature, reported in Fig.2. The optimal tuning has been performed by changing also the pressure acting on the QP and observing in the far field the quality of the Laguerre-Gauss modes generated. In this way it has been possible to choose the optimal tuning for all devices, hence maximizing the efficiency of each QP.

3. EXPERIMENTAL SETUP

The experimental layout is shown in Fig. 2. The source of the experiment is a Ti:Sa mode-locked laser with wavelength (wl) $\lambda = 795nm$, pulse duration of 180 fs, and repetition rate 76 MHz. The main part of the laser through a second harmonic generation (SHG) generates a UV laser beam with wave-vector k_p and power equal to $800mW$. This field pump a $1.5mm$ thick non-linear crystal of β-barium borate (BBO) cut for type II phase-matching that works in a collinear regime and generates polarization pairs with orthogonal polarization $\{\overrightarrow{\pi}_H, \overrightarrow{\pi}_V\}$ with equal wavelength $\lambda = 795nm$. The spatial and temporal walk-off is compensated through a $\frac{\lambda}{2}$ waveplate and a 0.75 mm thick BBO (C).[25] The photons are spectrally filtered adopting a broadband filter with $\Delta\nu = 6nm$. In order to work in the one or two photon regime, a polarizing beam-splitter (PBS) can be inserted in order to transmit the horizontally-polarized photon of the pair and reflects the vertically-polarized one. In the case of single-photon regime (PBS inserted), the vertically-polarized photon is coupled to a single-mode fiber and revealed with a single-photon counter (SPCM) D_T, which therefore acts as a trigger of the one-photon state

generation. The transmitted photon in the $|H\rangle$ polarization state is coupled to another single-mode fiber, which selects only a pure TEM_{00} transverse mode, corresponding to OAM $m = 0$. The coincidence count rate of the two outputs of the PBS, after coupling into the fibers, is of typically 16-18 kHz. After the output of the fiber, two waveplates compensate the rotation of polarization introduced by the fiber. So far we have described the

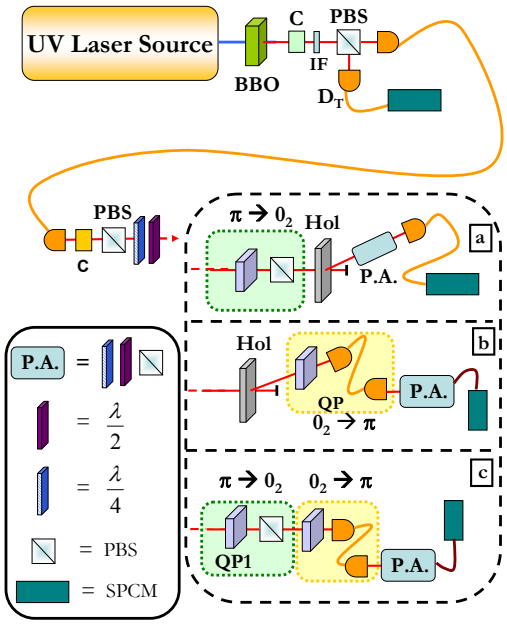

Figure 3. Experimental setup. The output signals of the single photon counter modules (SPCM) are sent to a coincidence box interfaced with a computer, which collects the different coincidence rates.

first part of the apparatus concerning the source of single photon states or two photon states depending on the experiment to be implemented. The second part of the experimental setup which has been changed depending on the different experiments (denoted as **a**, **b**, **c**) to be implemented, will be described in the following Sections.

4. MANIPULATION OF OAM QUBIT VIA Q-PLATES

In the next subsections we will describe the experiments we have carried out in order to demonstrate the reliability of the q-plate device on the manipulation of the orbital angular momentum. In this work we adopted, beyond the q-plate, also the hologram devices. The holograms used for generating or analyzing the above OAM states were manufactured from a computer-generated image by a photographic technique followed by a chemical bleaching step, producing pure phase binary holographic optical elements. The typical first-order diffraction efficiencies of these holograms were in the range 10-15%. Depending on the OAM basis to be analysed, the hologram is characterized by a different pattern. However, a TEM_{00} input mode is sent into the hologram and the first-order diffracted mode is used for output which depends on each hologram pattern. For example, let us consider a double-fork hologram like the one we used in our experiments. Such hologram separates the different values of the OAM, so that the first diffracted modes refer to $\Delta m = \pm 2$ respect to the value of OAM of the input beam, while the undiffracted beam is characterized by $\Delta m = 0$.

A single q-plate (with $q = 1$) can be used for coupling the polarization subspace π with the OAM subspace o_2, spanned by the OAM eigenstates $\{|+2\rangle_o, |-2\rangle_o\}$. Let us note that as the action of a single q-plate allows to work in a bidimensional subspace of the orbital angular momentum, it is possible to construct a "Poincaré"

sphere for an OAM qubit analogous to the one usually constructed for a polarization qubit.[26] Being $\{|+2\rangle, |-2\rangle\}$ the basis in the OAM subspace o_2, we define the following superposition states:

$$\begin{aligned} |d_R\rangle &= \frac{1}{\sqrt{2}}(|+2\rangle + |-2\rangle) \\ |d_L\rangle &= \frac{1}{i\sqrt{2}}(|+2\rangle - |-2\rangle) \\ |d_+\rangle &= \frac{1}{\sqrt{2}}(|d_R\rangle + |d_L\rangle) \\ |d_-\rangle &= \frac{1}{\sqrt{2}}(|d_R\rangle - |d_L\rangle) \end{aligned}$$

which enlighten the full analogy that can be drawn between the polarization SU(2) Hilbert space and each subspace of OAM with a given $|m|$, except for $m = 0$.

In the next subsections, we present two optical schemes based on the q-plate that enable a qubit of quantum information to be transferred from the polarization to the OAM (setup **a**, *transferrer* $\pi \rightarrow o_2$), from OAM to polarization (setup **b**, *transferrer* $o_2 \rightarrow \pi$). Moreover, we tested also the combination of these two schemes, thus realizing the *bidirectional transfer* polarization-OAM-polarization (setup **c**, $\pi \rightarrow o_2 \rightarrow \pi$). The latter demonstration is equivalent to demonstrating quantum communication using OAM for encoding the message. In other words, the qubit is initially prepared in the polarization space, then passed to OAM in a transmitting unit (Alice), sent to a receiving unit (Bob), where it is transferred back to polarization for further processing or detection. Let us stress that here we demonstrate a probabilistic conversion ($p = 50\%$) of these quantum transferrer. However by extending the following scheme it is possible to achieve a complete deterministic information conversion.[27]

4.1 Entanglement

The q-plate device allows to manipulate efficiently the OAM degree of freedom by coupling the OAM with the polarization of single photons. Interestingly, observing the dynamics shown in eq.1, emerges a first property of the QP that is to generate single particle entanglement between the π and o degrees of freedom:

$$\left.\begin{matrix} |H\rangle_\pi |0\rangle_o \\ |V\rangle_\pi |0\rangle_o \end{matrix}\right\} \overset{QP}{\rightarrow} \frac{1}{\sqrt{2}}(|L\rangle_\pi |+2\rangle_o \pm |R\rangle_\pi |-2\rangle_o) \tag{2}$$

Hence as a first experimental step in the single photon regime, we have demonstrated the realization of the states in Eq.(2). A single-photon two-qubit quantum state tomography has been carried out, performing measurements both in π and o degrees of freedom. In particular, different basis of the OAM have been analysed through six holograms with different diffraction patterns.[29] The experimental results are in very good agreement with theoretical predictions, as shown in Fig.(4-**a,b**). The average experimental concurrence is $C = (0.95 \pm 0.02)$, while the average purity of the states is $P = Tr\rho^2 = (0.94 \pm 0.02)$.

4.2 Quantum transferrer $\pi \rightarrow o_2$

Here we want to demonstrate that the q-plate enables to transfer the information encoded in the polarization degree of freedom to the OAM.

Let us consider as initial state the polarization-encoded qubit

$$|\Psi\rangle_{\text{in}} = |\varphi\rangle_\pi |0\rangle_o = (\alpha|H\rangle_\pi + \beta|V\rangle_\pi)|0\rangle_o \tag{3}$$

where $|0\rangle_o$ indicates the TEM_{00} mode. By passing it through a pair of suitably oriented quarter-waveplates, the photon state is rotated into the L, R basis:

$$(\alpha|L\rangle_\pi + \beta|R\rangle_\pi)|0\rangle_o \tag{4}$$

After the QP the quantum state of the photon is then turned into the following:

$$\alpha|R\rangle|+2\rangle+\beta|L\rangle|-2\rangle \tag{5}$$

If a polarizer along the horizontal direction is used, we then obtain the state

$$|\Psi\rangle_{out}=|H\rangle_{\pi}(\alpha|+2\rangle_{o}+\beta|-2\rangle_{o})=|H\rangle_{\pi}|\varphi\rangle_{o_2} \tag{6}$$

which completes the conversion. We note that such conversion process is probabilistic, since the state $|\Psi\rangle_{out}$

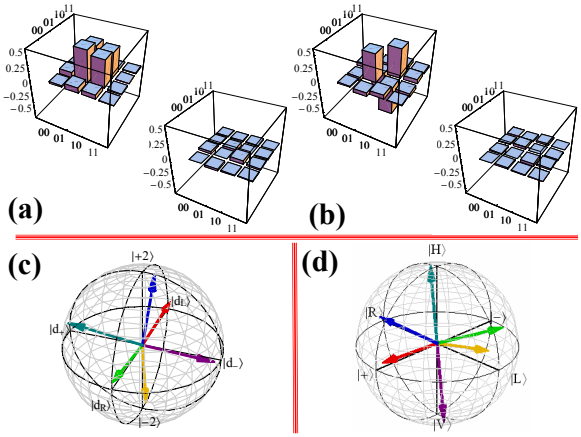

Figure 4. **(a-b)**Experimental density matrices for the single photon entangled state. The computational values $\{0,1\}$ are associated to the $\{|R\rangle,|L\rangle\}$ polarization states, and to $\{|+2\rangle,|-2\rangle\}$ for the orbital angular momentum m for the first and the second qubit, respectively. The incoming state on the QP is (**a**) $|H\rangle_{\pi}|0\rangle_{m}$, and (**b**) $|V\rangle_{\pi}|0\rangle_{m}$.**(c-d)**Poincaré sphere both for the OAM **(c)** and m **(d)** degrees of freedom. Experimentally we carried out single-qubit tomography in order to determine the Stoke's parameters for the π and their analogous for l degrees of freedom. The mean fidelity values are **(c)** $F=(98\pm1)\%$ and **(d)** $F=(97\pm1)\%$.

is obtained with a probability $p=50\%$, owing to the final polarizing step. Moreover, since we are using the $\{|H\rangle,|V\rangle\}$ basis for the polarization encoding and the $\{|+2\rangle,|-2\rangle\}=\{|m\rangle,|r\rangle\}$ for the OAM one, the transfer is associated also with a rotation of the Poincaré sphere. The experimental layout of this scheme is shown in Fig.3, dashed box **a**. The input arbitrary qubit is written in the polarization using two waveplates, and the final state tomography has been realized by means of the six holograms properly patterned. The experimental results for three specific choices of the input state are shown in Fig.(4-**c**). We find a good agreement with theory as demonstrated by the fidelity parameter, defined as $F=\langle\psi|\rho_{exp}|\psi\rangle$, where $|\psi\rangle$ is the theoretical state to be compared to the experimental one. Hence in this experiment the average fidelity value between the experimental states and the theoretical predictions is $F=(97.7\pm0.2)\%$.

Thus, we have demonstrated experimentally that the initial information encoded in an input TEM_{00} state can be coherently transferred to the OAM degree of freedom, thanks to the $\pi\rightarrow o_2$ transferrer, giving rise to the preparation of a qubit in the orbital angular momentum.

4.3 Quantum transferrer $o_2\rightarrow\pi$

Let us now show that the reverse process can be realized as well, by transferring a qubit initially encoded in the OAM subspace o_2 into the polarization space. We therefore consider as initial quantum state of the photon the following one:

$$|\Psi\rangle_{\mathrm{in}}=|H\rangle_{\pi}|\varphi\rangle_{o_2}=|H\rangle(\alpha|+2\rangle+\beta|-2\rangle) \tag{7}$$

By injecting the state $|\Psi\rangle_{in}$ in the q-plate device, and then rotating the output state by means of a pair of waveplates, we obtain the following state:

$$\frac{1}{2}\{\alpha|V\rangle|+4\rangle+\alpha|H\rangle|0\rangle+\beta|V\rangle|0\rangle+\beta|H\rangle|-4\rangle\} \tag{8}$$

Now, by coupling the beam to a single mode fiber, only the states with $m = 0$ that is, the TEM_{00} modes, will be efficiently transmitted. Of course, this implies that a probabilistic process is obtained again, since we discard all the contributions with $m \neq 0$ (ideally, again $p = 50\%$). After the fiber, the output state reads:

$$|\Psi\rangle_{out} = (\alpha|H\rangle + \beta|V\rangle)|0\rangle = |\varphi\rangle_{\pi}|0\rangle_{o} \tag{9}$$

which demonstrates the successful conversion from the OAM degree of freedom to the polarization one.

The experimental layout of this "reverse" scheme is shown in Fig.3, dashed box **b**. The input qubit in OAM is prepared using one of the six holograms, as explained in the previous subsection. The output state has been analyzed by a standard polarization-state quantum tomography. The experimental results for three cases are shown in Fig.(4-**d**). We find again a good agreement with theory, with an average fidelity $F = (97.3 \pm 0.2)\%$

4.4 Bidirectional transfer $\pi \rightarrow o_2 \rightarrow \pi$

Having demonstrated polarization-to-OAM transfer and OAM-to-polarization transfer, it is natural to try both schemes together, in a bidirectional transfer which starts and ends with polarization encoding, with OAM as an intermediate state which can be used for example for communication. This is also the first quantum experiment based on the combined use of two q-plates. Hence we verify that the efficiency of the optical manipulation is not strongly affected by the number of q-plate employed, for example due to alignment criticality.

The layout is shown in Fig.3, dashed box **c**, and corresponds to the sequence of the two schemes discussed above. In Fig.5 we show some density matrices obtained by the quantum tomography technique in the polarization degree of freedom of the output state. The experimental results are in good agreement with the theoretical

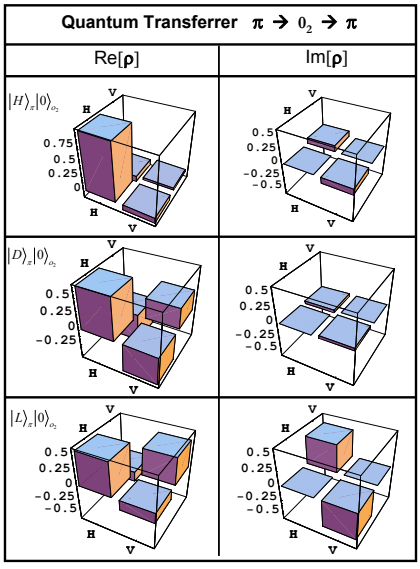

Figure 5. Experimental density matrices measured in the polarization degree of freedom after the bidirectional $\pi \rightarrow o_2 \rightarrow \pi$ transferrer. In each box is reported the expression of the initial and final state, to be compared with the experimental one described by the density matrix.

predictions, with a mean fidelity value equal to $F = (95.9 \pm 0.2)\%$.

Let us now address the efficiency of the system based on two sequential q-plates, that is the transferrer $\pi \rightarrow o_2$ followed by the analysing q-plate. The conversion efficiency η of the single QP is quite high, around 85%, and can reach $\eta \sim 90\%$ if properly tuned. Hence one would expect a total efficiency close to 76%, which however can be lowered by a factor $\alpha = (0.5 \div 0.7)$ related to the mismatch in the alignment of the two q-plates. As a matter of

fact, if the topological singularities of the sequential q-plate are not perfectly matched, the Laguerre-Gauss mode generated by the first QP can not be completely converted, hence analysed, by the second QP. Experimentally, the total efficiency has been extimated to be tipically around $(40 \div 50)\%$.

5. HONG-OU-MANDEL EFFECT

We have demonstrated that the QP allows to manipulate efficiently the OAM degree of freedom, and represents a reliable interface between polarization π and OAM o and *viceversa*. As a first demonstration of the QP quantum properties in the two-photon regime, we address here the experimental observation of the two-photon coalescence, the so-called Hong-Ou-Mandel (HOM) effect, in the OAM degree of freedom.

Quantum interference using a pair of correlated photons has played an important role in the recent developments of quantum information and fundamental studies of quantum nonlocality. Such phenomenon has been exploited for quantum teleportation,[30–32] construction of quantum logic gates for processing of quantum information,[33–35] optimal cloning of a quantum state[36–38] and various other applications.

The experimental setup adopted for the HOM experiment is shown in Fig.6. As we carried out a two-photon experiment, after the photon source reported in Fig.3, we removed the PBS and D_T, which act as a trigger of the one-photon state generation. After the single mode fiber we separeted the photons on two spatial modes a and b through a polarizing beam splitter. Both on modes a and b we insert a transferrer $\pi \rightarrow o_2$. On the balanced

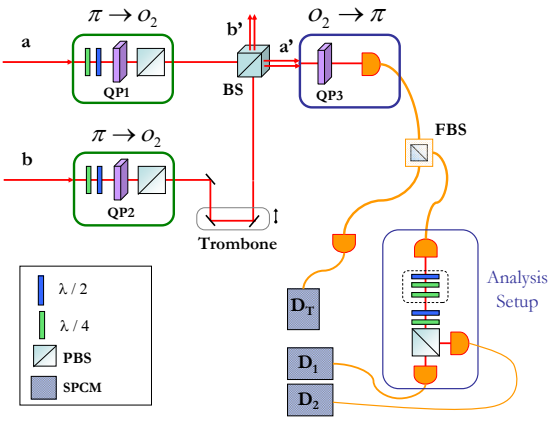

Figure 6. Experimental setup implemented for the Hong-Ou-Mandel experiment in the OAM degree of freedom.

beam splitter BS we let shine the two photons carrying the information in the OAM degree of freedom after the $\pi \rightarrow o_2$ transferrer. The trombone device and the polarizing beam splitters guarantee the perfect temporal match and the same polarization state of the two photons so they should yield the standard HOM effect. However we manipulate also the OAM degree of freedom so we expect to observe the interference between the two photons only if they are in the same OAM state. In order to analyse the quantum state encoded in the OAM degree of freedom, we insert a $o_2 \rightarrow \pi$ transferrer based on QP3. The photons coupled in the single mode fiber are separated through a fiber integrated BS and then analysed in polarization with a standard analysis setup.

The first measure has been performed by preparing both on arms a and b the same OAM state. In particular we have let interfere on the BS the state $|H\rangle_\pi| - 2\rangle_o$. As expected by theory, we have found a peak in the coincidence counts. In order to demonstrate that the Hong-Ou-Mandel effect observed is related to a pure quantum OAM effect, we have performed the same measurement by preparing two orthogonal states in the OAM degree of freedom on arms a and b. The experimental results are shown in Fig.7. Even though the photons injected on the beam splitter have the same polarization and temporal delay, no interference occur, since the orbital component of their wavefunction differs. Theoretically, the interference of the two photons should lead to a coincidence enhancement by a factor $R = 2$, and the coincidence counts enhancement observed in this Hong-Ou-Mandel experiments reads $R = (1.98 \pm 0.05)$. Such experiment is related to the factorization of the input

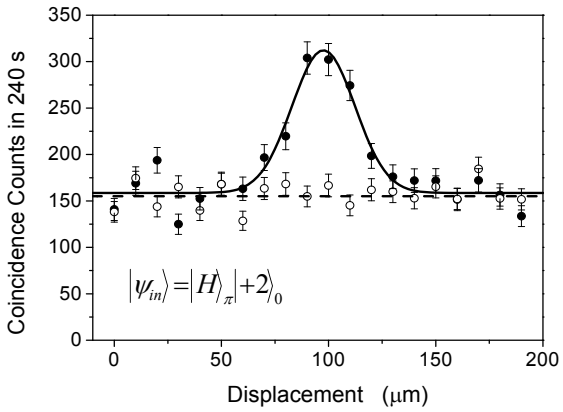

Figure 7. Experimental results of the Hong-Ou-Mandel coalescence in the OAM degree of freedom. Injection on the BS of the same LG state (black spots) and orthogonal LG states (empty spots). The solid curve represents the best fit based on theoretical prediction.

qubit wavefunction in three contributions: spatial, spinoarial and orbital. In particular we have proved that the orbital wavefunction can be deterministically manipulated and contributes towards interference phenomena like the spinorial one.

6. CONCLUSIONS AND PERSPECTIVES

The orbital angular momentum represents a promising resource for high dimensional quantum information protocols yet to be completely exploited. At the same time the development of new devices able to manipulate efficiently and deterministically the OAM degree of freedom has opened new perpectives. Here we have presented a recently developed device known as *q-plate*, which allows to easily manipulate the OAM degree of freedom with an efficiency higher than the one usually associated to the more popular hologram tecnique. In particular, we have demonstrated that the q-plate is a reliable interface between OAM and polarization, able to coherently transfer the information from the polarization to the OAM degree of freedom and *viceversa*. Exploiting the "spin-to-orbit" coupling that takes place in the q-plate, here we have also experimentally carried out the observation of a two-photon Hong-Ou-Mandel coalescence related to the OAM properties of the photon's wavefunctions.

This work contributes towards the employment of the OAM in quantum information protocols, enlightening the efficiency of the q-plate technique. Apart for the basic conceptual relevance of this demonstration, the reliability of our approach is expected to pave the way towards a complete, deterministic control of the photon's orbital angular momentum for quantum information applications. Specifically it would be possible to implement logic gates as C-NOT gates, and different quantum information protocols like purification and quantum cloning.

REFERENCES

1. Allen, L., Beijersbergen, M. W., Spreeuw, R.J.C., & Woederman,J.P., "Orbital Angular Momentum of light and the transformation of Laguerre-Gaussian modes", *Physical Review A* **45**, 8185 (1992).
2. Molina-Terriza, G., Torres, J.P., & Torner, L., "Twisted photons", *Nature Physics* **3**, 305 (2007).
3. Franke-Arnold, S., Allen, L., and Padgett, M. J., "Advances in optical angular momentum", *Laser and Photonics* **2**, 299 (2008).
4. Bruss, D., "Optimal Eavesdropping in Quantum Cryptography with Six States", *Phys. Rev. Lett.* **81**, 3018 (1998).
5. Fujiwara, M., Takeoka, M., Mizuno, J., and Sasaki, M., "Exceeding the Classical Capacity Limit in a Quantum Optical Channel", *Phys. Rev. Lett.* **90**, 167906 (2003).

6. Torner, L., Torres, J. P., and Carrasco, S., "Digital spiral imaging", *Opt. Expr.* **13**, 873 (2005).
7. Berkhout, G. C. G., and Beijersbergen, M. W., "Method for probing the orbital angular momentum of optical vortices in electromagnetic waves from astronomical objects", *Phys. Rev. Lett.* **101**, 100801 (2008).
8. Galajda, P., and Ormos, P., "Complex micromachines produced and driven by light", *Appl. Phys. Lett.* **78**, 249 (2001).
9. Saleh, B. E. A., and Teich, M. C., *Fundamentals of Photonics*, J.W. Goodman Editor.
10. Mair, A., Vaziri, A., Weihs, G., and Zeilinger, A., "Entanglement of the orbital angular momentum of photons", *Nature (London)* **412**, 313 (2001).
11. Molina-Terriza, G., Torres, J. P.,& Torner, L., "Orbital angular momentum of photons in noncollinear parametric downconversion", *Optics Communication* **228**, 115 (2003).
12. Vaziri, A., Pan, J. W., Jennewein, T., Weihs, G., and Zeilinger, A., "Concentration of Higher Dimensional Entanglement: Qutrits of Photon Orbital Angular Momentum", *Phys. Rev. Lett.* **91**, 227902 (2003).
13. Arnaut, H., and Barbosa, G. A., "Orbital and Intrinsic Angular Momentum of Single Photons and Entangled Pairs of Photons Generated by Parametric Down-Conversion", *Phys. Rev. Lett.*, **85**, 286 (2000).
14. Franke-Arnold, S., Barnett, S. M., Padgett, M. J., and Allen, L., "Two-photon entanglement of orbital angular momentum states", *Phys. Rev. A* **65**, 033823 (2002).
15. Aiello, A., Oemrawsingh, S. S. R., Eliel, E. R., and Woerdman, J. P., "Nonlocality of high-dimensional two-photon orbital angular momentum states", *Phys. Rev. A* **72**, 052114 (2005).
16. Vaziri, A., Weihs, G., and Zeilinger, A., "Experimental Two-Photon, Three-Dimensional Entanglement for Quantum Communication" *Phys. Rev. Lett.* **89**, 240401 (2002).
17. Stutz, M., Greblacher, S., Jennewein, T., Zeilinger, A., "How to create and detect N-dimensional entangled photons with an active phase hologram", *Appl. Phys. Lett.* **90**, 261114 (2007).
18. Barreiro, J. T., Langford, N. K., Peters, N. A., & Kwiat, P.G., "Generation of Hyperentangled photons pairs", *Phys. Rev. Lett.* **95**, 260501 (2005).
19. Barreiro, J. T., Wei, T. C., and Kwiat, P. G., "Beating the channel capacity limit for linear photonic superdense coding", *Nature Physics* **4**, 282 (2008).
20. Marrucci, L., Manzo, C., and Paparo, D., "Optical Spin-to-Orbital Angular Momentum Conversion in Inhomogeneous Anisotropic Media", *Physical Review Letters* **96**, 163905 (2006).
21. Marrucci, L., Manzo, C., and Paparo, D., "Pancharatnam-Berry phase optical elements for wave front shaping in the visible domain: Switchable helical mode generation", *Applied Physics Letters* **88**, 221102 (2006).
22. Stalder, M., and Schadt, M., "Linearly polarized light with axial symmetry generated by liquid-crystal polarization converters", *Opt. Lett.* **21**, 1948 (1996).
23. Nagali, E., Sciarrino, F., De Martini, F., Marrucci, L., Piccirillo, B., Karimi, E., and Santamato, E., "Quantum interference by coherence transfer from spin to orbital angular momentum of photons", *quant-phys arXiv:*0810.2417 (2008).
24. Calvo, G. F., and Picon, A., "spin-induced angular momentum switching", *Opt. Lett.* **32**, 7 (2007).
25. Kwiat, P. G., Mattle, K., Weinfurter, H., Zeilinger, A., Sergienko, A. V., and Shih, Y. H., "New high-intensity source of polarization-entangled photon pairs",*Phys. Rev. Lett.* **75**, 4337 (1995).
26. Padgett, M. J., and Courtial, J., "Poincaré-sphere equivalent for light beams containing orbital angular momentum",*Opt. Lett.*, **24**, 430 (1999).
27. Nagali, E., Sciarrino, F., De Martini, F., Marrucci, L., Piccirillo, B., Karimi, E., and Santamato, E., "Polarization control of single photon quantum orbital angular momentum states", *quant-phys arXiv:*0902.0740 (2009).
28. Hong, C. K., Ou, Z. Y., and Mandel, L., "Measurement of subpicosecond time intervals between two photons by interference", *Physical Review Letters* **59**, 2044 (1987).
29. Langford, N. K., et al., "Measuring Entangled Qutrits and Their Use for Quantum Bit Commitment", *Physical Review Letters* **93**, 053601 (2004).
30. Bouwmeester, D., Pan, J. W., Mattle, K., Eibl, M. , Weinfurter, H., and Zeilinger, A., "Experimental quantum teleportation", *Nature (London)* **390**, 575 (1997).

31. Boschi, D., Branca, S., De Martini, F., Hardy, L., and Popescu, S., "Experimental Realization of Teleporting an Unknown Pure Quantum State via Dual Classical and Einstein-Podolsky- Rosen Channels", *Phys. Rev. Lett.* **80**, 1121 (1998).
32. Lombardi, E., Sciarrino, F., Popescu, S., and De Martini, F., "Teleporation of a Vacuum-One-Photon Qubit", *Phys. Rev. Lett.* **88**, 070402 (2002).
33. Pittman, T. B., Fitch, M. J., Jacobs, B. C., and Franson, J.D., "Experimental controlled-NOT logic gate for single photons in the coincidence basis", *Phys. Rev. A* **68**, 032316 (2003).
34. OBrien, J. L., et al., "Demonstration of an alloptical quantum controlled-NOT gate", *Nature (London)* **426**, 264 (2003).
35. Gasparoni, S., Pan, J. W., Walther, P., Rudolph, T., and Zeilinger, A., "Realization of a Photonic Controlled-NOT Gate Sufficient for Quantum Computation", *Phys. Rev. Lett.* **93**, 020504 (2004).
36. Irvine, W. T. M., Linares, A. L., de Dood, M. J. A., and Bouwmeester, D., "Optimal Quantum Cloning on a Beam Splitter", *Phys. Rev. Lett.***92**, 047902 (2004).
37. Gisin, N., and Massar, S., "Optimal Quantum Cloning Machines", *Phys. Rev. Lett.* **79**, 2153 (1997).
38. Ricci, M., Sciarrino, F., Sias, C., and De Martini, F., "Teleportation scheme implementing the Universal Optimal Quantum Cloning Machine and the Universal NOT gate", *Phys. Rev. Lett.* **92**, 047901 (2004).
39. De Martini, F., and Sciarrino, F., "Non-linear Parametric Processes in Quantum Information", *Progress in Quantum Electronics* **29**, 165-256 (2005).
40. Aolita, L., and Walborn, S. P., "Quantum Communication without Alignment using Multiple-Qubit Single-Photon States", *Phys. Rev. Lett.* **98**, 100501 (2007).